

# Temperature-scanned magnetic resonance and the evidence of two-way transfer of a nitrogen nuclear spin hyperfine interaction in coupled NV-N pairs in diamond

R. A. Babunts\*, A. A. Soltamova\*, D. O. Tolmachev\*<sup>1)</sup>, V. A. Soltamov\*, A. S. Gurin\*, A. N. Anisimov†, V. L. Preobrazhenskii\*, P. G. Baranov\*†

\*Ioffe Physical-Technical Institute, 194021 St.-Petersburg, Russia

†St.-Petersburg State Polytechnical University, 195251 St.-Petersburg, Russia

Submitted 20 March 2012

New method for the detection of magnetic resonance signals versus temperature is developed on the basis of the temperature dependence of the spin Hamiltonian parameters of the paramagnetic system under investigation. The implementation of this technique is demonstrated on the nitrogen-vacancy (NV) centers in diamonds. Single NV defects and their ensembles are suggested to be almost inertialess temperature sensors. The hyperfine structure of the <sup>14</sup>N nitrogen nuclei of the nitrogen-vacancy center appears to be resolved in the hyperfine structure characteristic to the hyperfine interaction between NV and N<sub>s</sub> center (substitutional nitrogen impurity) in the ODMR spectra of the molecular NV–N<sub>s</sub> complex. Thus, we show that a direct evidence of the two-way transfer of a nitrogen nuclear spin hyperfine interaction in coupled NV–N<sub>s</sub> pairs was observed. It is shown that more than 3-fold enhancement of the NV ODMR signal can be achieved by using water as a collection optics medium.

**1. Introduction.** The nitrogen-vacancy (NV) defect in diamond consists of a nitrogen substituting for a carbon plus a nearest-neighbor vacancy. The NV defect is the only known solid-state system where manipulation of the spin states of a single localized electron was realized at room temperature [1–3]. In optical absorption and emission the NV defect gives rise to a zero-phonon line (ZPL) at 637 nm and a structured phonon side-band (PSB). Upon optical excitation a strong spin alignment is generated in the triplet <sup>3</sup>A ground state with the zero-field splitting (ZFS) of 2870 MHz and as a result optically detected magnetic resonance (ODMR) in the NV defect ground state can be observed by monitoring the photoluminescence (PL) intensity. Due to a strong thermal isolation of the NV defect spin system from the diamond lattice, nonequilibrium distribution of the populations between spin sublevels is determined by the optical pumping process, and not by spin-lattice relaxation. NV defect in diamond is one of the most prominent objects for Applications [4]. NV defects have been effectively generated in diamond by irradiation and following high temperature annealing [5]. Enormously high concentrations of NV defects were shown [6] to be produced directly through high-pressure high-temperature (HPHT) sintering of detonation nanodiamonds.

**2. Experimental.** The samples we used in our studies were commercial high-pressure high-tempera-

ture (HPHT) grown micron and millimeter size bulk diamonds with initial nitrogen concentration of 100 ppm. Samples were subjected to irradiation by either electrons or neutrons at a dose of 10<sup>18</sup> cm<sup>-2</sup> and then annealed at 800 °C; concentration of the NV centers in irradiated and annealed samples was about 10 ppm according to the EPR measurements. ODMR was measured at 2.5–3 GHz region in zero and low magnetic fields in the temperature range from 77 K up to 600 K. The ODMR spectra were recorded using standard methods: by scanning the frequency or magnetic field. In addition a new method of detection of the ODMR was developed and discussed in this paper: ODMR spectra were recorded by scanning the temperature at a fixed frequency and a fixed magnetic field. The basis for the development of this method is the presence of at least several spin Hamiltonian parameters sensitive to the temperature, e.g., axial (*D*) and transverse (*E*) ZFS constants.

**3. Results and discussion.** Fig. 1 shows the zero-field ODMR spectra of the NV defects measured at 25 and 260 °C by monitoring the ZPL at 637 nm and phonon sideband intensities of the NV centers excited by 532 nm laser. The spectra were recorded by frequency scanning at two temperatures and have practically same shape, but are shifted by about 30 MHz. The spectra exhibit two intense central lines that can be described by the standard spin Hamiltonian with the ZFS constants of *D* = 2870 MHz and *E* = 3.5 MHz at 25 °C and *D* = 2842.5 MHz and *E* = 3.1 MHz at 260 °C.

<sup>1)</sup>e-mail: Daniel.Tolmachev@gmail.com

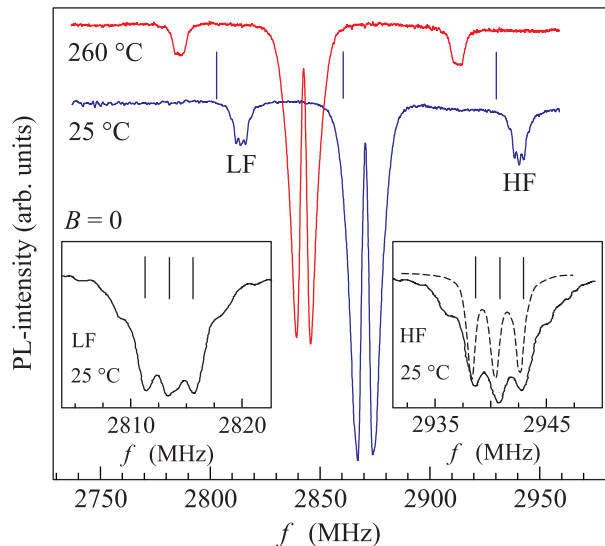


Fig. 1. Zero-field ODMR spectra of the NV defects and NV- $N_s$  pairs measured at 25 and 260 °C in  $n$ -irradiated and annealed diamond crystal; (insets) LF and HF sideband recorded in expanded scale at 25 °C; simulated spectrum for the NV central transition ( $E = 0$ ) with  $^{14}\text{N}$  hyperfine structure using the parameters of the Ref. [7]

In addition, two relatively weak sidebands shifted to the low-frequency (LF) and high-frequency (HF) sides from the main double transition were observed. The sidebands in expanded scale are presented in Figs. 1b and c. For the first time similar sidebands have been observed in bulk diamond crystals [8] and have been shown to arise from the interaction between triplet NV defect and substitutional nitrogen atom  $N_s$ , which is a deep donor in the neutral charge state with a net spin of  $S = 1/2$  (coupled triplet-doublet molecular NV- $N_s$  pair in diamond) and related to the strong hyperfine (HF) interaction with the substitutional nitrogen nuclei  $^{14}\text{N}_s$ .

Unique feature of the spectra observed is the additional splittings resolved in the sidebands (Fig. 1) that are observed for the first time to the best of our knowledge. The sideband itself is related to the HF interaction between the substitutional  $N_s$  and the NV centers as was discussed. Additional splitting resolved in these lines can be assigned to the weak HF interaction between  $N_s$  substitutional atoms and  $^{14}\text{N}$  nuclei in the NV defect. The magnitude of this splitting is identical to the HF splitting, which was observed directly in the NV defect [7]. A simulated spectrum for the NV central transition ( $E = 0$ ) with  $^{14}\text{N}$  hyperfine structure using the parameters of Ref. [7] is submitted for comparison in the same frequency scale (Fig. 1, dashed line).

Following the Ref. [8], the spin Hamiltonian describing the coupled triplet-doublet (NV- $N_s$ ) spin system (when the quadrupole interaction is neglected) is

$$H = g_1\mu_B\mathbf{B} \cdot \mathbf{S}_1 + D[S_{1Z}^2 - 2/3] + E[S_{1X}^2 - S_{1Y}^2] + \mathbf{S}_1 \cdot \hat{A}_1 \cdot \mathbf{I}_1 + g_2\mu_B\mathbf{B} \cdot \mathbf{S}_2 + \mathbf{S}_2 \cdot \hat{A}_2 \cdot \mathbf{I}_2 + \mathbf{S}_1 \cdot \hat{T} \cdot \mathbf{S}_2, \quad (1)$$

where  $\mu_B$  is the Bohr magneton, for the NV defect:  $S_1 = 1$ ,  $D$  and  $E$  are the ZFS constants ( $D = 2870$  MHz and  $E = 3.5$  MHz at 25 °C),  $g_1$  is the isotropic electron-spin  $g$ -factor ( $g_1 = 2.0028$ ),  $\hat{A}_1$  is the HF coupling tensor describing the HF interaction with the  $^{14}\text{N}$  in the NV center ( $A_{1\parallel} = 2.14$  MHz and  $A_{1\perp} = 2.70$  MHz [9]); for  $N_s$  donor:  $S_2 = 1/2$ ,  $g_2$  is the isotropic electron  $g$ -factor ( $g_2 = 2.0024$ ),  $\hat{A}_2$  is the HF tensor describing the HF interaction with the  $N_s$  center ( $A_{2\parallel} = 114.0$  MHz and  $A_{2\perp} = 81.3$  MHz [8]), and  $\hat{T}$  is the triplet-doublet NV- $N_s$  magnetic dipole-dipole interaction tensor ( $T = 10$  MHz [8]). The  $N_s$  HF splitting is transferred to the ODMR spectra of the NV defect. The presence of a nonzero parameter  $E$  results in the non-equidistant sidebands relative to the center of the spectrum (Fig. 1). It should be noted that the  $^{14}\text{N}$  HF interaction for the NV defect was not observed in Ref. [8] and therefore was not included in the spin Hamiltonian.

Fig. 1 shows a significant change of the  $D$  and  $E$  parameters with temperature. The majority of the triplet centers in diamond [10], and in SiC [11] exhibit strong temperature dependencies of  $D$  and  $E$ . In Ref. [12] the temperature dependence of the axial ZFS,  $D$ , of the NV defect ensemble was observed.

The temperature induced effects provide an opportunity to develop new methods of magnetic resonance detection. Fig. 2 shows the ODMR spectra of the NV- $N_s$  pairs recorded at zero magnetic field by scanning temperature from 25 to 250 °C. The measurements were performed at three fixed frequencies corresponding to the low frequency sides of the ODMR lines recorded at 25 °C (marked by vertical bars in Fig. 1). The resonance lines should move to the lower frequencies with the temperature increase from 25 to 250 °C. The central lines, LF and HF sidebands were recorded at fixed frequencies 2860, 2803 and 2931 MHz, respectively. It is seen that the central signal, LF and HF sidebands have the same temperature dependence, that is, this method of recording allows us to conclude that these spectra belong to the same paramagnetic molecular system – the fact that is not obvious from the standard ODMR spectra. Additional structure indicated by vertical bars is resolved in the temperature scanned ODMR spectra. As was discussed above this splitting is due to the strong HF interaction with the isolated substitutional  $N_s$  centers exhibiting the HF structure due to the weak HF interaction with the  $^{14}\text{N}$  nucleus in the NV defect.

The central part of the spectrum presented in Fig. 1 is shown for comparison in Fig. 2 (dashed line), the dis-

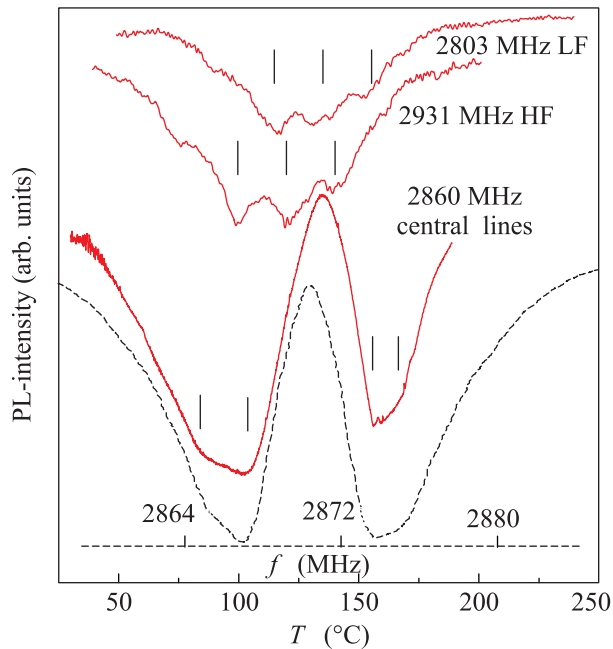


Fig. 2. Zero-field ODMR spectra of the NV defects and the NV- $N_s$  pairs, recorded in zero magnetic field at fixed frequencies indicated in Fig. 1 for 25 °C by scanning temperature; the central part of the 25 °C measured ODMR spectrum of Fig. 1 is presented for comparison by dashed line

tance between the two lines that are registered with the frequency and temperature scans are chosen the same, which corresponds to 125 kHz/°C. It is evident that both methods allow the registration of the similar signals with the additional splitting due to the  $^{14}\text{N}$  HF structure of the NV defect (see vertical bars). The width of two lines, being the same when the ODMR spectrum is recorded versus the frequency, differ significantly when recording is performed versus the temperature. High-temperature line is narrower indicating that with the increase of the sample temperature, the temperature induced change of the axial ZFS constant  $D$  increases. This temperature induced effects provide an unique opportunity for local registration of the small temperature changes with a nanoscale resolution using nanodiamonds with the NV centers as a probe.

To stabilize the temperature of the sample, we have placed the diamond sample with the NV defects directly into the water. The striking result is that the intensities of the PL and ODMR signals have more than tripled. Fig. 3 shows the zero-field ODMR spectra of the NV defects recorded at 25 °C in air and in water in  $n$ -irradiated and annealed diamond crystal.

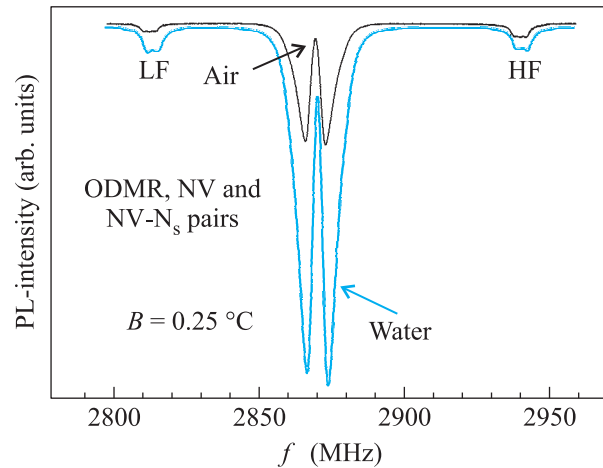


Fig. 3. Zero-field ODMR spectra of the NV defects recorded at 25 °C in air and water in  $n$ -irradiated and annealed diamond crystal

As a result of Snell's law, most of the PL is trapped inside the diamond matrix, since total internal reflection (TIR) is achieved as soon as a collection angle  $\theta > \theta_{\text{TIR}} = \arcsin(n_c/n_d)$ ;  $n_c$  and  $n_d$  are the refractive index of collection optics medium and diamond, respectively. For a diamond-air interface this limits the collection angle to  $\theta_{\text{TIR}} \sim 24.4^\circ$ , for a diamond-water interface  $\theta_{\text{TIR}} \sim 33.3^\circ$ . Using a 0.85-NA microscope objective, the collection efficiency was estimated [13] to be only 2.6% for a planar diamond surface in the air. One should expect that when the diamond is placed in the water the light emission efficiency from the diamond will enhance significantly due to increase of the  $\theta_{\text{TIR}}$ . It is effect that was observed by us and demonstrated in Fig. 3.

**4. Conclusion.** New method of magnetic resonance detection versus temperature based on the temperature dependence of the spin Hamiltonian parameters was developed. The proposed technique of temperature-scanned magnetic resonance is especially important when an EPR spectrum of paramagnetic impurities consists of many lines that belong to different centers with a different temperature dependences of the spin Hamiltonian parameters. In this case the method should allow the reliable distinguishability of the signals that belong to the different centers. We have demonstrated the application of this method to the NV defects in diamond and suggest that the single NV defect and their ensembles can be used as inertialess temperature sensors.

A well-resolved structure due to the hyperfine interaction with  $^{14}\text{N}$  nitrogen nuclei in the NV defects in diamond has been observed in the sidebands belonging to the HF structure of the substitutional nitrogen atom  $N_s$  in the zero-field ODMR spectra of the NV- $N_s$  mole-

cular complex. Thus, we have shown that there is direct two-way coherent transfer of a nitrogen nuclear spin HF interaction in coupled NV–N<sub>s</sub> pairs. More than 3-fold enhancement of the NV ODMR signal was achieved using water as collection optics medium.

This work has been supported by Ministry of Education and Science, Russia, under the Contracts # 14.740.11.0048 and 16.513.12.3007; the Programs of the Russian Academy of Sciences: “Spin Phenomena in Solid State Nanostructures and Spintronics”; “Fundamentals of nanostructure and nanomaterial technologies” and by the Russian Foundation for Basic Research.

- 
1. A. Gruber, A. Drbenstedt, C. Tietz et al., *Science* **276**, 2012 (1997).
  2. F. Jelezko, I. Popa, A. Gruber et al., *Appl. Phys. Lett.* **81**, 2160 (2002).
  3. P. Nizovtsev, S. Ya. Kilin, F. Jelezko et al., *Physica B: Cond. Mat.* **340–342**, 106 (2003).
  4. J. Wrachtrup, *PNAS* **107**, 9479 (2010) and references therein.
  5. J.-P. Boudou, P. A. Curmi, F. Jelezko et al., *Nanotechnology* **20**, 235602 (2009).
  6. P. G. Baranov, A. A. Soltamova, D. O. Tolmachev et al., *SMALL* **7**, 1533 (2011).
  7. F. Jelezko and J. Wrachtrup, *Phys. Stat. Sol. (a)* **203**, 3207 (2006).
  8. E. van Oort, P. Stroomeer, and M. Glazbeek, *Phys. Rev. B* **42**, 8605 (1990).
  9. S. Felton, A. M. Edmonds, M. E. Newton et al., *Phys. Rev. B* **79**, 075203 (2009).
  10. Y. M. Kim, Y. H. Lee, P. Brosious, and J. W. Corbet, *Proc. Intern. Conf. on Radiation Damage and Defects in Semiconductors*, Reading, England, 1972, Institute of Physics, London (1973), p. 202.
  11. N. M. Pavlov, M. I. Iglitsyn, M. G. Kosaganova, and V. N. Solomatin, *Sov. Phys. Semicond.* **9**, 845 (1976).
  12. V. M. Acosta, E. Bauch, M. P. Ledbetter et al., *Phys. Rev. Lett.* **104**, 070801 (2010).
  13. P. Siyushev, F. Kaiser, V. Jacques et al., arXiv:1009.0607v1 [quant-ph] 3 Sep 2010.